Supporting Information

Allostery in a disordered protein: Oxidative modifications to α-Synuclein act distally to regulate membrane binding

Eva Sevcsik, Adam J. Trexler, Joanna M. Dunn, and Elizabeth Rhoades

Methods

Protein labeling. For fluorescence correlation spectroscopy (FCS) experiments, aS was labeled with Alexa Fluor 488 (AL488) (Invitrogen, Carlsbad, CA) at residue 9 in Tris buffer (20 mM Tris, 130 mM NaCl, pH 7.4). UV-Vis absorbance at 495 nm was used to quantify the AL488 concentration, but was insufficiently sensitive for determination of aS concentration due to the large absorbance of AL488 ($\varepsilon=7800$ $M^{-1}cm^{-1}$) and the lower absorbance of aS ($\varepsilon=5120$ $M^{-1}cm^{-1}$ for wild-type; this value is lower for mutants lacking some or all of the tyrosines) at 280 nm. The final protein concentration was determined by a modified Lowry assay (Bio-Rad, Hercules, CA). Labeling efficiencies were consistently between 85 and 95%. Double labeling for single molecule Förster resonance energy transfer (smFRET) measurements was achieved by reacting aS sequentially with acceptor fluorophore, Alexa Fluor 594 (AL594), and donor fluorophore, AL488, in Tris buffer following a protocol described previously.[1] This fluorophore pair is expected to have a Förster radius, the distance at which the probability of energy transfer occurring is 50%, of ~54 Å.[2] Fluorescence anisotropy measurements showing similar rotational freedom of both dyes at all labeling positions rule out site-specific labeling artifacts (Table S1). Fluorescence lifetime measurements were made of each of the dyes at each of the labeling positions (Table S1).

Nitration. Nitration of aS was achieved by adding a 10x molar excess of tetranitromethane (TNM) (10% in ethanol) per tyrosine residue to 2 mg/mL fluorescently labeled aS. Labeling was done prior to nitration to avoid possible modification of free cysteine residues. The mixture was stirred vigorously for one hour, with a second bolus of TMN added after 30 minutes. Excess TNM was removed on a Zeba Spin Desalting column (Thermo Scientific, Rockford, IL).

Nitration of aS yields a heterogeneous mixture of different aS species.[3] In addition to nitrated monomers, dimers and higher oligomers are formed due to di-tyrosine cross-linking. Monomeric nitrated aS (nit-aS) was separated from oligomers and dimers on a Sephacryl 200 size exclusion column (GE Healthcare Life Sciences, Pittsburgh, PA), and its purity confirmed by SDS-PAGE (Figures S1 and S2). The nitration profile of monomeric nit-aS was determined by ESI mass spectrometry (Table S2).

Preparation of lipid vesicles. Stock solutions of 1-Palmitoyl-2-oleoyl-*sn*-glycero-3-phospho-L-serine (POPS) and 1-palmitoyl-2-oleoyl-*sn*-glycero-3-phosphocholine (POPC) (Avanti Polar Lipids, Alabaster, AL) were prepared in chloroform and stored at -20°C. Aliquots were mixed, dried under a stream of nitrogen and stored in vacuum for at least 4 hours to remove residual chloroform. Lipid films were hydrated in Tris buffer at room temperature for 1 hour with

intermittent vigorous vortexing. Large unilamellar vesicles (LUVs) were prepared by extrusion of lipid suspensions through two stacked 50 nm diameter Nucleopore Track-Etch membranes (Whatman Inc., Clifton, NJ) using a Lipofast apparatus (Avestin Inc., Ottawa, Canada). The final lipid concentration of the extruded vesicles was determined using a total phosphorus assay.[4,5] For FCS binding measurements, POPC/POPS 1/1 vesicles were used. In order to ensure that the protein was mostly bound, POPS vesicles were used for smFRET experiments (the K_D for unmodified aS for 100% POPS vesicles in 130 mM NaCl is ~8 µM [6]).

Fluorescence correlation spectroscopy. FCS measurements were made on a lab-built instrument based around an Olympus IX71 inverted microscope and a 488nm DPSS laser as described previously.[1] Laser power was adjusted to 5 µW prior to entering the microscope. Fluorescence emission was collected through the objective and separated from laser excitation using a Z488rdc long pass dichroic and an HQ600/200m bandpass filter (Chroma, Bellows Falls, VT) and focused onto the aperture of a 50 µm optical fiber (Oz Optics, Ottawa, Canada) directly coupled to an avalanche photodiode (Perkin Elmer, Waltham, MA). A digital correlator (Flex03LQ-12, correlator.com, Bridgewater, NJ) was used to generate the autocorrelation curve.

FCS measurements were made in 8-well chambered coverglasses (Nunc, Rochester, NY) passivated by polylysine conjugated polyethylene glycol treatment to prevent aS adsorbtion to the chamber surface. Binding studies were made by titrating 1:1 POPC/POPS vesicles to 100 nM aS in Tris buffer. For each FCS measurement 25 traces of 10 seconds each were recorded and averaged together to obtain statistical variations. A measurement time of 10 seconds for individual curves was chosen because it is ~1800 times longer than the diffusion time of the vesicles, and thus within the required range to obtain accurate measurements of diffusion time.[7] We have previously confirmed the suitability of this measurement time by increasing the measurement time for individual curves to 30 seconds and found that it did not result in any changes in the autocorrelation curves or calculated fit parameters.[8] The average curve was fit to the following equation for multiple species of differing brightness (Equation 1) weighted by the inverse of the experimentally determined variance [9] using MATLAB (The MathWorks, Natick, MA):

$$G(\tau) = \frac{\sum_i Q_i^2 N_i g_i}{\left(\sum_i Q_i N_i\right)^2} \qquad \text{Equation 1}$$

Where Q_i is the brightness of the ith species relative to species 1, N_i is the number of molecules of species i in the focal volume, and g_i is the autocorrelation function of species i.

For two species (free protein and vesicle-bound protein) diffusing in three dimensions through a diffraction limited focal volume, this equation becomes:[10]

$$G(\tau) = \frac{1}{N}\left(F_F * \frac{1}{1+\dfrac{\tau}{\tau_{aS}}} * \sqrt{\frac{1}{1+\dfrac{s^2\tau}{\tau_{aS}}}} + Q*(1-F_F)*\frac{1}{1+\dfrac{\tau}{\tau_{vesicle}}} * \sqrt{\frac{1}{1+\dfrac{s^2\tau}{\tau_{vesicle}}}} \right)$$ Equation 2

where s is the ratio of radial to axial dimensions of the focal volume, determined to be 0.2 for our system, and τ_{aS} and $\tau_{vesicle}$ are the diffusion times of aS and vesicles, respectively, which were measured independently and fixed for binding measurements. τ_{aS} was obtained from an aS-only solution, while the highest lipid concentration of the titration was used for $\tau_{vesicle}$ since little free protein is expected at that point. These data were fit to an equation for one-component diffusion to obtain τ_{aS} and $\tau_{vesicle}$ (Equation 3).

$$G(\tau) = \frac{1}{N} * \frac{1}{1+\dfrac{\tau}{\tau_D}} * \sqrt{\frac{1}{1+\dfrac{s^2\tau}{\tau_D}}}$$ Equation 3

Binding measurements were fit using Equation 2. The only free parameters were N, the number of proteins, F_F, the fraction of aS free in solution, and Q, the average brightness of the vesicles relative to a single aS.

Binding curves were generated by plotting the fraction of bound protein against the concentration of accessible lipid. Two lipid concentrations were chosen from intermediate points in the binding curves, where the fraction of bound protein can be determined with highest accuracy, and molar partition coefficients K_P were calculated as described previously [8] using Equation 4.

$$K_P = \frac{[aS_{lipid}]}{[aS_{buffer}]} = \frac{[aS_{bound}]*\dfrac{V_{buffer}}{V_{lipid}}}{[aS_{buffer}]}$$ Equation 4

where K_P is the molar partition coefficient, aS_{lipid} is the moles of aS per volume of lipid and aS_{buffer} is the moles of free aS per volume of aqueous solution. Individual K_p values were averaged and a standard error of the mean was taken as the uncertainty. The free energy of binding is calculated as: $\Delta G = -RTln(K_P)$, where R is ideal gas constant and T is temperature.

Single-molecule FRET. For smFRET experiments, laser power was adjusted to 15-25 µW just prior to entering the microscope. Fluorescence emission was collected through the objective, and donor and acceptor photons were separated by a HQ585LP dichroic mirror (Chroma, Bellows Falls, VT), and then further selected using band-pass filters: ET 525/50M for the donor, HQ600LP for the acceptor (Chroma, Bellows Falls, VT) and detected by avalanche photodiodes coupled through 100 µm diameter aperture optical fibers (Oz Optics, Ottawa, Canada). Photon traces for the acceptor and donor channels were collected in 1 ms time bins.

Energy transfer efficiency (ET_{eff}) values were calculated for protein bursts as $ET_{eff} = (I_a - \beta * I_d) / (I_a + \gamma * I_d)$. β accounts for donor fluorescence bleed-through to the acceptor channel (0.06 for Alexa Fluor 488 in our system with the filters described above). γ accounts for differences in detection efficiency and quantum yield for the fluorophores and has been determined to be $\gamma = 1.2$ for this system [1]. For every protein construct, at least three independent photon traces yielding several thousand events were measured, the ET_{eff} values were calculated and compiled into a histogram.

In order to discriminate photon bursts arising from protein from background noise, we employed a threshold scheme by selecting the number of photons at which the highest signal:noise ratio was obtained. This threshold was calculated by comparing photon traces of buffer in the absence and presence of protein. We employed a sum (sum of donor and acceptor channels) threshold to discriminate protein events from background.

PGF-NMR data collection and analysis. For each sample, 20 spectra were collected with the strength of the diffusion gradient increasing from 1.69 to 33.72 Gauss/cm in a linear manner. Signals from 0 to 0.5 ppm were integrated using the MestReNova software (Mestrelab Research, Santiago de Compostela, Spain) and diffusion data were fitted to Gaussian functions using Origin software to give the apparent diffusion coefficients. Sodium-3-trimethylsilylproprionate (TMSP) was used as an internal standard to calculate R_H of the protein. R_H values obtained in at least three independent experiments were averaged and a standard error of the mean was taken as the uncertainty. The hydrodynamic radius (R_H) of TMSP was determined to be 3.43 ± 0.1 Å using the known R_H of dioxane (2.12 Å) [11] in five independent measurements.

Calculation of distances from smFRET measurements. In order to convert the mean measured ET_{eff} values to distances, we modeled aS as a Gaussian chain with an end-to-end probability function in the form of: $P(r) = 4\pi r^2 \left(\frac{3}{2\pi \langle r^2 \rangle} \right) exp - \left(\frac{3r^2}{2\langle r^2 \rangle} \right)$, where r is the end-to-end distance of the protein chain, and $\langle r^2 \rangle$ is the root-mean-square end-to-end distance.[12] The mean energy transfer efficiency, $\langle E \rangle$, can be expressed as: $\langle E \rangle = \int_0^\infty \frac{1}{1 + \left(\frac{r}{R_o} \right)^6} * P(r)$, where R_o for our donor-acceptor pair is 54 Å. We solved this equation numerically for $\langle r^2 \rangle$ using *Mathematica*, and then converted $\langle r^2 \rangle$ to radius of gyration, R_g by: $R_g = \sqrt{\frac{\langle r^2 \rangle}{6}}$.

Anisotropy. Steady state fluorescence anisotropy measurements were made at all labeling positions to ensure that fluorophore rotation was not significantly hindered by interactions with the protein. Given that random fluorescent dipole orientation is a key assumption in FRET, we wanted to ensure that no one position in aS restricted fluorophore motion more than any other. We previously measured AL488 and AL594 at positions 9, 33, 54, 72 and 92 and found similar rotation for these fluorophores at each position.[1,13] For the current study, measurements were repeated with aS labeled at position 115. A QuantaMaster C-61 fluorescence spectrometer (PTI) was used for all measurements, and fluorescence emission intensity was collected for 60 seconds and the average value was used for calculations. The G factor was calculated by measuring free AL488 or AL594 dye by $G = I_{hv}/I_{hh}$. Fluorescence intensity was measured for 50 nM aS in Tris

buffer. Anisotropy (r) was calculated as $r = \dfrac{I_{vv} - G * I_{vh}}{I_{vv} + 2 * G * I_{vh}}$. Anisotropy values are listed in Table S1. We observed that AL488 had a lower average anisotropy than AL594, which is expected given the larger size and increased hydrophobicity of AL594. All anisotropy values were < 0.15, which indicates that rotational constraint should not introduce significant artifacts into our FRET measurements.[14]

Fluorescence lifetime measurements. Fluorescence lifetime data for all labeling positions except position 115 have been published previously.[1,13] Measurements for position 115 were performed on a fluorolog TCSPC fluorometer (Horiba Jobin Yvon, Edison, NJ). A 459 nm NanoLED and a 566 nm NanoLED were used to excite AL488 and AL594, respectively. Before the measurements, an instrument response decay was collected for each NanoLED using a scattering solution (LUDOX LS colloidal silica). 2μM aS labeled with either AL488 or AL594 was then measured until 10,000 events were detected, and the distribution of lifetimes from this measurement was fit using one or two exponential decays. Values are listed in Table S1.

Circular Dichroism. CD spectra of unmodified and nit-aS were measured in an Applied Photophysics Chirascan (Surrey, United Kingdom). The protein concentration was ~15 μM for both constructs, in 20 mM phosphate buffer, pH 7.4, with 50 mM NaCl. Five spectra were measured with 1 nm resolution and averaged to obtain the curves shown. Buffer curves were measured independently and subtracted from the protein spectra.
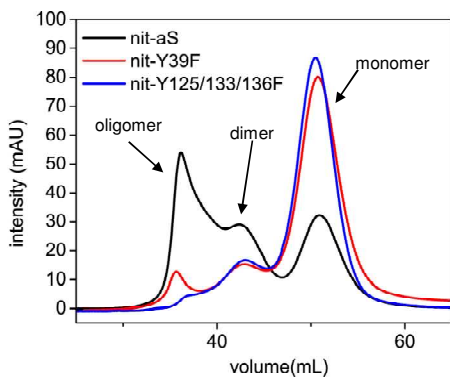
Supporting Information Figures

Figure S1. Size exclusion chromatograms of nitrated aS and Y→F mutants. Both the nitrated Y39F (red) and Y125/133/136F (blue) mutants show considerably less dimer and oligomeric species than nit-aS (black) suggesting that inter-molecular cross-linking is most efficient if it involves Y39 and one of the C-terminal tyrosines. This observation is in agreement with a previous study showing that at least one tyrosine on each end of the protein is required for di-tyrosine cross-linking mediated aggregation.[15]
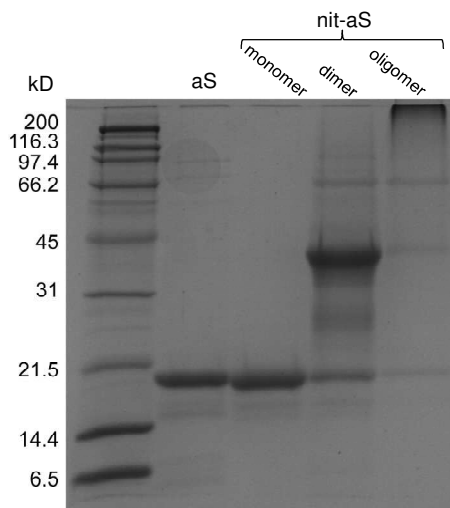
Figure S2. SDS-PAGE of unmodified aS and nitrated monomer, dimer and oligomer fractions, showing that a clean fraction of nitrated monomer aS can be obtained from separation on a Sephacryl 200 column.
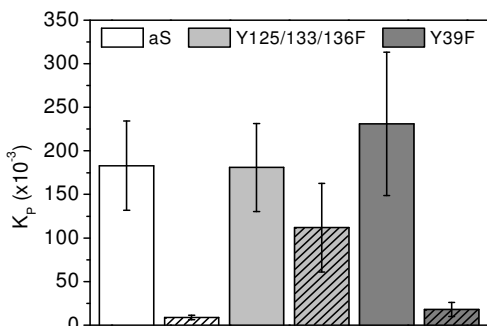

Figure S3. Partition coefficients of the different aS Y→F constructs at pH 5.0, wild-type (white), Y125/133/136F (light gray), and Y39F (dark gray). Unmodified constructs are solid, nitrated constructs have diagonal hatch marks. The partition coefficient of unmodified aS is 7-fold higher at pH 5.0 (~51,000) than at pH 7.4 (~7,000). This increased affinity for anionic vesicles is due to the decreased negative charge of aS at pH 5.0. At pH 7.4 the net charge of aS is -9, and +5 for the N-terminal membrane binding region, whereas at pH 5.0 the total net charge is -3, and +8 for the membrane binding region (its calculated pI is at 4.7). This increase of positive charges in the membrane binding region outweighs the decreased negative charge density of the lipid bilayer (the carboxyl group of POPS is 50% negatively charged at pH 5.0 as compared to fully negatively charged at pH 7.4 [16,17]). At pH 5.0, nitrotyrosine is uncharged [18], thus, any charge-related effects of tyrosine nitration on membrane-binding should be eliminated, as seen in the case of the Y125/133/136F mutant. In contrast, the Y39F construct shows the same decrease in binding affinity as the wild-type protein, indicating that the reduction in affinity is not due to electrostatic repulsion.
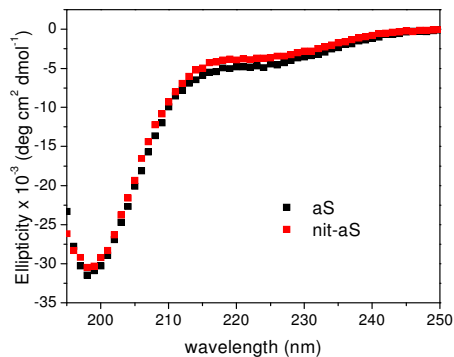
Figure S4. Circular dichroism of aS (black) and nit-aS (red). Although there are minor differences between the two spectra, there is no evidence of stable secondary or tertiary structure as a result of nitration. The spectra of both proteins suggest a primarily random structure.
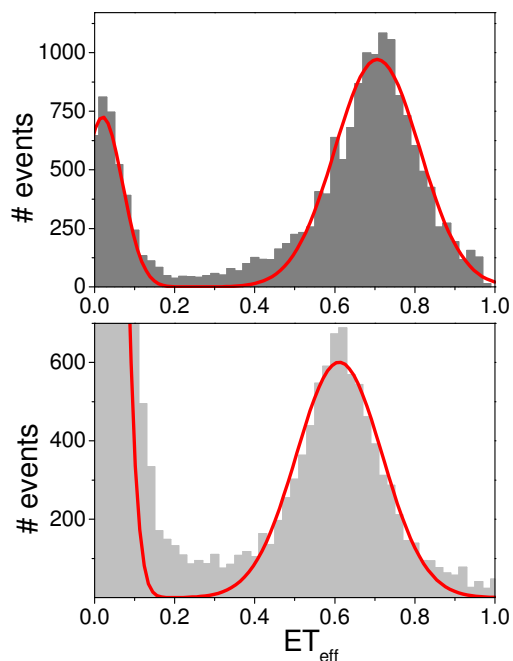

Figure S5. smFRET of Y125/133/136D labeled at positions 72 and 115 in buffer (upper, dark gray) and bound to vesicles (lower, light gray). The peak positions (ET_{eff}~0.7 in buffer and ET_{eff}~0.6 on vesicles) are comparable to those measured for the unmodified protein (Figure 3I and K) and distinct from those observed for the nitrated protein (Figure 3J and L).
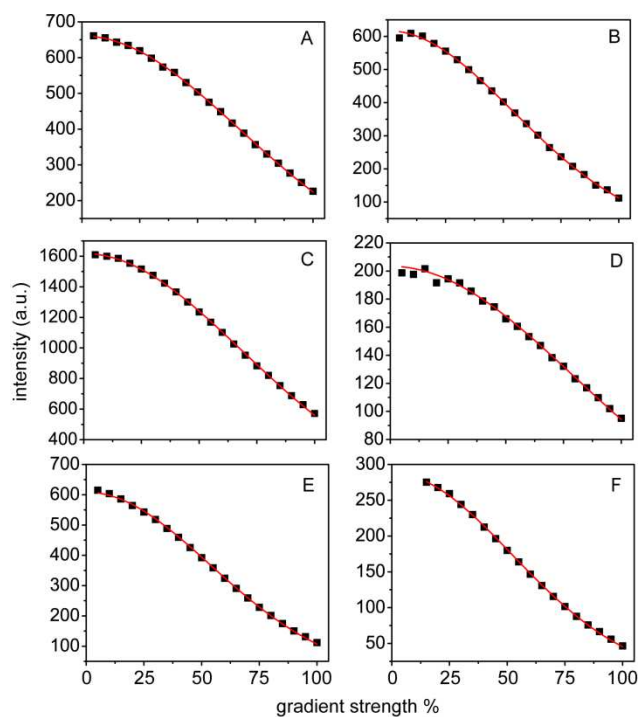
Figure S6. Signal intensity vs gradient strength plots of PFG-NMR data. A, C and E. aS, nit-Y39F and Y125/133/136D in buffer. B, D and F. aS, nit-Y39F and Y125/133/136D in 8M urea. Fits are shown in red.

Supporting Information Tables

Table S1. Anisotropy and fluorescence lifetime of singly labeled constructs.*

	AL488		AL594	
position	Anisotropy (AU)	Lifetimes (ns)	Anisotropy (AU)	Lifetimes (ns)
9	0.066	3.9 (94%), 1.9(6%)	0.137	4.4
33	0.090	3.9 (94%), 1.6 (6%)	0.123	4.4
54	0.074	4 (93%), 2.5 (7%)	0.120	4.4
72	0.059	4.2	0.119	4.4
92	0.035	4.2 (96%), 7.6 (4%)	0.096	4.4
115	0.102	4.1 (76%), 2.7 (25%)	0.099	4.17

*All anisotropy and lifetime values except for position 115 have been previously published in SI Reference 11.

Table S2. Predicted and measured masses of the different aS constructs after nitration and separation from di- and oligomeric species.

	Nitrated	Expected mass	Measured mass	Estimated %
nit-aS	0	14460	14460±5	0
	1	14505	14505±3	15
	2	14550	14550±0	35
	3	14595	14595±1	35
	4	14640	14640±1	15
nit-Y39F	0	14444	14447±1	10
	1	14489	14491±1	30
	2	14534	14536±1	30
	3	14579	14582±5	30
nit-Y125/133/136F	0	14412	-	0
	1	14457	14460±1	100

Table S3. Diffusion times of unmodified and nitrated constructs determined by FCS.

	Diffusion times (ms)	
	unmodified	nitrated
aS	0.510±0.006	0.531±0.006
Y39F	0.518±0.006	0.536±0.008
Y125/33/136F	0.508±0.011	0.497±0.009

Supporting Information References
(1)   Trexler, A. J.; Rhoades, E. *Biochemistry* **2009**, *48*, 2304-2306.
(2)   Schuler, B.; Lipman, E. A.; Eaton, W. A. *Nature* **2002**, *419*, 743-747.
(3)   Hodara, R.; Norris, E. H.; Giasson, B. I.; Mishizen-Eberz, A. J.; Lynch, D. R.; Lee, V. M.; Ischiropoulos, H. *J. Biol. Chem.* **2004**, *279*, 47746-47753.
(4)   Fiske, C. H.; Subbarow, Y. *J. Biol. Chem.* **1925**, *66*, 375-400.
(5)   Chen, P. S.; Toribara, T. Y.; Warner, H. *Anal. Chem.* **1956**, *28*, 1756-1758.
(6)   Rhoades, E.; Ramlall, T. F.; Webb, W. W.; Eliezer, D. *Biophys. J.* **2006**, *90*, 4692-4700.
(7)   Reis, J.; Schwille, P. *Phys. Chem. Chem. Phys.* **2008**, *10*, 3487-3497.
(8)   Middleton, E. R.; Rhoades, E. *Biophys. J.* **2010**, *99*, 2279-2288.
(9)   Wohland, T.; Rigler, R.; Vogel, H. *Biophys. J.* **2001**, *80*, 2987-2999.
(10)   Rauer, B.; Neumann, E.; Widengren, J.; Rigler, R. *Biophys. Chem.* **1996**, *58*, 3-12.
(11)   Jones, J. A.; Wilkins, D. K.; Smith, L. J.; Dobson, C. M. *J. Biomol. NMR* **1997**, *10*, 199-203.
(12)   O'Brien, E. P.; Morrison, G.; Brooks, B. R.; Thirumalai, D. *J. Chem. Phys.* **2009**, *130*, 124903.
(13)   Trexler, A. J.; Rhoades, E. *Biophys. J.* **2010**, *99*, 3048-3055.

(14)   McCarney, E. R.; Werner, J. H.; Bernstein, S. L.; Ruczinski, I.; Makarov, D. E.; Goodwin, P. M.; Plaxco, K. W. *J. Mol. Biol.* **2005**, *352*, 672-682.

(15)   Ruf, R. A.; Lutz, E. A.; Zigoneanu, I. G.; Pielak, G. J. *Biochemistry* **2008**, *47*, 13604-13609.

(16)   MacDonald, R. C.; Simon, S. A.; Baer, E. *Biochemistry* **1976**, *15*, 885-891.

(17)   Cevc, G.; Watts, A.; Marsh, D. *Biochemistry* **1981**, *20*, 4955-4965.

(18)   Sokolovsky, M.; Riordan, J. F.; Vallee, B. L. *Biochemistry* **1966**, *5*, 3582-3589.

Complete References from Manuscript with truncated Author Lists

(3)   Cooper, A. A.; Gitler, A. D.; Cashikar, A.; Haynes, C. M.; Hill, K. J.; Bhullar, B.; Liu, K.; Xu, K.; Strathearn, K. E.; Liu, F.; Cao, S.; Caldwell, K. A.; Caldwell, G. A.; Marsischky, G.; Kolodner, R. D.; Labaer, J.; Rochet, J. C.; Bonini, N. M.; Lindquist, S. *Science* **2006**, *313*, 324-328.

(4)   Paleologou, K. E.; Oueslati, A.; Shakked, G.; Rospigliosi, C. C.; Kim, H. Y.; Lamberto, G. R.; Fernandez, C. O.; Schmid, A.; Chegini, F.; Gai, W. P.; Chiappe, D.; Moniatte, M.; Schneider, B. L.; Aebischer, P.; Eliezer, D.; Zweckstetter, M.; Masliah, E.; Lashuel, H. A. *J. Neurosci.* **2010**, *30*, 3184-3198.

(5)   Polymeropoulos, M. H.; Lavedan, C.; Leroy, E.; Ide, S. E.; Dehejia, A.; Dutra, A.; Pike, B.; Root, H.; Rubenstein, J.; Boyer, R.; Stenroos, E. S.; Chandrasekharappa, S.; Athanassiadou, A.; Papapetropoulos, T.; Johnson, W. G.; Lazzarini, A. M.; Duvoisin, R. C.; Di Iorio, G.; Golbe, L. I.; Nussbaum, R. L. *Science* **1997**, *276*, 2045-2047.

(14)   Singleton, A. B.; Farrer, M.; Johnson, J.; Singleton, A.; Hague, S.; Kachergus, J.; Hulihan, M.; Peuralinna, T.; Dutra, A.; Nussbaum, R.; Lincoln, S.; Crawley, A.; Hanson, M.; Maraganore, D.; Adler, C.; Cookson, M. R.; Muenter, M.; Baptista, M.; Miller, D.; Blancato, J.; Hardy, J.; Gwinn-Hardy, K. *Science* **2003**, *302*, 841.